Journal of Frontiers in Multidisciplinary Research

Theoretical Investigation of Charge-Transfer Kinetics at the MK-2 Dye/InP Semiconductor Interface

Mohsin A Hassooni
Department of Physics, College of Education for Pure Science -Ibn Al-Haitham, University of Baghdad, Baghdad, Iraq

* Corresponding Author: **Mohsin A Hassooni**

Article Info

E-ISSN: 3050-9726
P-ISSN: 3050-9718
Volume: 07
Issue: 02
Received: 16-12-2026
Accepted: 14-10-2026
Published: 12-11-2026
Page No: 444-451

Abstract
Interfacial charge transfer from a photoexcited sensitizer to a semiconductor conduction band is a key process governing the performance of dye/semiconductor photoelectrodes. In this work, the charge-transfer kinetics at the MK-2 dye/InP interface were investigated theoretically using a nonadiabatic Marcus–Gerischer electron-transfer model that explicitly incorporates the conduction-band density of states of InP. The reorganization energy (λ_{AD}) was calculated from the dielectric and refractive-index properties of the MK-2 dye, the InP semiconductor, and four solvent environments - N,N-dimethylacetamide (DMAc), acetonitrile (ACN), methanol (MeOH), and 2,2,2-trifluoroethanol (TFE) - yielding values between 0.344 and 0.408 eV. The driving force for electron injection, ΔV^0, was obtained as −0.83 eV from the energetic offset between the MK-2 excited-state potential and the InP conduction-band edge, and the corresponding conduction-band density of states was evaluated as D_0(E) = 1.326 × 10^{20} eV^{-1} cm^{-3} at this energy. The charge-transfer rate (R_{CT}^{DA}) was computed as a function of the electronic coupling parameter (V_{DA}, 0.10–0.40 eV) for each solvent. R_{CT}^{DA} was found to scale with $|V_{DA}|^2$, consistent with nonadiabatic electron-transfer theory. Because $|\Delta V^0|$ exceeds λ_{AD} in all four solvents, the system lies in the Marcus inverted region, so R_{CT} increases with increasing λ_{AD} (TFE > MeOH > ACN > DMAc), contrary to the trend expected in the normal Marcus regime. These results indicate that the interfacial charge-transfer rate at the MK-2/InP interface is controlled jointly by electronic coupling strength, solvent-dependent reorganization energy relative to the fixed driving force, and the finite density of accepting states in the InP conduction band

DOI: https://doi.org/10.54660/.JFMR.2026.7.2.444-451

Keywords: charge transfer, dye/semiconductor, MK-2 dye, InP semiconductor

Introduction

Charge-transfer reactions involve the movement of an electron from an electron donor to an electron acceptor and play an important role in a wide range of optical [1], electronic [2], and sensing applications [3]. At heterojunction interfaces, the interaction between materials with different electronic structures can strongly influence charge separation and transport. Electrostatic interactions and interfacial charge-transfer forces can also affect the organization and electronic behavior of donor–acceptor systems [4]. The combination of two dissimilar materials in a heterojunction may therefore provide physical and chemical properties that are not present in the individual components [5]. In such systems, the energetic separation between the initial and final electronic states is one of the parameters that governs the feasibility and kinetics of charge transfer [6].

Photoinduced charge transfer is particularly important at dye–semiconductor interfaces, where photoexcitation of the sensitizer can be followed by electron injection into available electronic states of the semiconductor. MK-2 is a metal-free donor–π–acceptor organic dye developed for dye-sensitized solar-cell applications. Its molecular structure consists of a carbazole-based electron-donor group and a cyanoacrylic-acid electron-acceptor and anchoring group connected through an oligothiophene

π-conjugated bridge [7]. Experimental studies on MK-2-sensitized semiconductor systems have also shown that electron-injection dynamics are sensitive to the local interfacial environment, indicating that the nature of the dye–semiconductor contact can directly affect charge-transfer kinetics [8].

Indium phosphide (InP) provides a semiconductor acceptor in which injected electrons can access a continuum of electronic states rather than a single discrete acceptor level. Theoretical treatments of semiconductor/liquid interfaces have previously applied Fermi's golden rule to InP and other semiconductors by accounting for transitions involving semiconductor electronic states and molecular redox states [9, 10]. This distinction is important because the charge-transfer rate at a molecular–semiconductor interface is influenced not only by the energetic driving force but also by electronic coupling, nuclear and solvent reorganization, temperature, and the availability of semiconductor states at the relevant injection energies.

Marcus theory provides a useful framework for describing electron-transfer processes in donor–acceptor systems [11]. In the classical discrete-state description, the rate depends on the driving force and reorganization energy, and sufficiently large exergonic driving forces can lead to the Marcus inverted region, where a further increase in driving force reduces the rate [12].

The earlier studies has examined in electronic transfer at Dye contact with InP interfaces depending on electronic structure calculations [13],

while many research investigate the electronic properties of MK-2 and other dyes with semiconductor [14] .

In this study, a theoretical investigation of charge transfer introduces at the MK-2 dye/InP interface. Although previous studies investigate charge transfer at interfaces and the electronic properties of dyes, these studies establish the charge-transfer characteristics of the particular MK-2/InP system. This work focused on the energetic alignment between the MK-2 dye and the InP semiconductor, with taken attention to the alignment of the relevant electronic energy levels and the influence of density of states on the calculated charge-transfer rate.

Previous investigations have examined the photovoltaic performance and interfacial electron-transfer behavior of MK-2 mainly in metal-oxide-based dye-sensitized systems [7, 8], while theoretical studies of semiconductor interfaces, including InP, have shown that semiconductor electronic structure plays an important role in determining interfacial electron-transfer kinetics [9, 10]. On this basis, the present work theoretically investigates charge-transfer kinetics at the MK-2 dye/InP semiconductor interface. The analysis is formulated within a Fermi-golden-rule/Marcus framework in which electron injection from the photoexcited dye is treated through the energy-resolved conduction-band states of InP. Particular attention is given to the roles of the driving energy, reorganization energy, and semiconductor-state availability in determining the calculated charge-transfer rate.

Theory

The charge transfer rate CTR for the elementary charge transfer process CT under resonant conditions can be calculated within the framework of Fermi's golden rule by considering that the charge transfer occurs between two donor and acceptor electronic states for a non-radiative transition. The charge transfer rate CTR is defined as [15]

$$R_{CT}^{DA}(\epsilon) = \frac{2\pi}{\hbar}\Gamma(\Delta\,\epsilon_{AD}, T) \quad (1)$$

Where $\Gamma(\Delta\,\epsilon_{AD}, T)$ is the Fermi's golden function, defined by [16].

$$\Gamma(\Delta\,\epsilon_{AD}, T) = |\langle F|\hat{H}|I\rangle|^2 \sum_{v_1}\sum_{v_2} P_v(T)\langle v_1|v_2\rangle\delta(\epsilon_D - \epsilon_A - \Delta\epsilon_{DA}) \quad (2)$$

Where $\hat{H}$ is electronic coupling operators for CT reaction from Initial state I in donor to final state F in acceptor, $P_v(T)$ is Boltzmann population, $v_1$and v_2 are vectors of the vibrational donor and acceptor quantum states, respectively, ϵ_D and ϵ_A are the donor and acceptor energies, respectively. The first term in Eq. (2) is indicated to the electronic coupling matrix element for charge transfer reaction and given by [10].

$$|\langle V_{DA}\rangle|^2 = |\langle F|\hat{H}|I\rangle|^2 \quad (3)$$

Inserting equation (3) in equation (2) to give

$$\Gamma(\Delta\,\epsilon_{AD}, T) = |\langle V_{DA}\rangle|^2 \sum_{v_1}\sum_{v_2} P_v(T)\langle v_1|v_2\rangle\delta(\epsilon_D - \epsilon_A - \Delta\epsilon_{DA}) \quad (4)$$

And the effective density of state $\rho_e(\Delta\epsilon_{DA}, T)$ is given by

$$\rho_e(\Delta\epsilon_{DA}, T) = \sum_{v_1}\sum_{v_2} P_v(T)\langle v_1|v_2\rangle\delta(\epsilon_D - \epsilon_A - \Delta\epsilon_{DA}) \quad (5)$$

Inserting equations (3), (4) in equation (1) to obtained

$$R_{CT}^{DA}(\epsilon) = \frac{2\pi}{\hbar}|\langle V_{DA}\rangle|^2\rho_e(\Delta\epsilon_{DA}, T) \quad (6)$$

The the effective density of state $\rho_e(\Delta\epsilon_{DA}, T)$for donor-acceptor system is written as [17]

$$\rho_e(\Delta\epsilon_{DA}, T) = \int_{-\infty}^{\infty} \boldsymbol{\mathcal{p}}(\Delta\epsilon_{DA}, T)\,\zeta(\Delta\epsilon_{DA} - \epsilon)dE \quad (7)$$

where $\boldsymbol{\mathcal{p}}(\Delta\boldsymbol{E}, \boldsymbol{T})$ is the density of state and $\zeta(\Delta\boldsymbol{E} - \boldsymbol{E})$ is the spectral distributions of the donor - acceptor electron attachment. The density of state distributions for system is [18]

$$\mathcal{p}(\Delta\mathrm{E}, \mathrm{T}) = \frac{1}{\sqrt{4\pi\lambda_{AD}\mathrm{k_B T}}} e^{\frac{-(\lambda_{AD}+\Delta V^0+\epsilon)^2}{4\lambda_{AD}k_B T}} \quad (8)$$

Where λ_{AD} and $\Delta V^0$are reorganization energy and driving energy. The reorganization energy$\lambda_{AD}(eV)$ can be defined by [19]

$$\lambda_{AD}(eV) = \frac{q^2}{8\pi\varepsilon^\circ}\left[\frac{\varepsilon - n^2}{\varepsilon n^2 R} - \frac{1}{2D}\left[\frac{1}{n^2}\frac{n_A^2 - n^2}{n_A^2 + n^2} - \frac{1}{\varepsilon^2}\frac{\varepsilon_A^2 - \varepsilon^2}{\varepsilon_A^2 + \varepsilon^2}\right]\right] \quad (9)$$

Here q ,ε° and R refers to charge, permittivity and radius, n ,ε and D are refractive index , dielectric constant and interfacial separation between donor and acceptor, n_A and ε_A are refractive index and dielectric constant of acceptor. The radius R estimates via density ρ,molecule weight M and Avogadros constant N using formula [20].

$$R(A^0) = 0.620\left(\frac{M}{N\rho}\right)^{\frac{1}{3}} \quad (10)$$

The spectral distributions $\zeta(\Delta\epsilon_{DA}-\epsilon)$ of the donor - acceptor electronic attachment relative to activation density of state for system $\varrho_{act}(E)$ and given by [21].

$$\zeta(\Delta\epsilon_{DA}-\epsilon)=\varrho_a(E)\frac{l_e}{\sqrt[3]{\frac{6d_a^2}{\pi}}} \quad (11)$$

Where l_e is length coupling in acceptor, d_a is the atomic density of acceptor. The electronic-state distribution $\varrho_a(E)$ must contain a density-of-states factor. Under the constant-DOS approximation, the acceptor density of states is assumed to vary negligibly over the energy window relevant to charge transfer:$D_a(E)\simeq D_0$,

Inserting equation (11) and equation (8) in equation (7) to secure

$$\rho_e(\Delta\epsilon_{DA},T)=\int_{-\infty}^{\infty}\frac{1}{\sqrt{4\pi\lambda_{AD}k_BT}}e^{\frac{-(\lambda_{AD}+\Delta V^0+\epsilon)^2}{4\lambda_{AD}k_BT}}\varrho_a(E)\frac{l_e}{\sqrt[3]{\frac{6d_a^2}{\pi}}}d\epsilon \quad (12)$$

Here, the semiconductor energy variable is defined relative to the InP conduction-band edge as $\epsilon=E-E_c, \varepsilon\geq 0$, so that $E=E_c+\epsilon$. Consequently, the physical integration domain is $0\leq\epsilon<\infty$. This change of lower limit is introduced by the energy reference $\epsilon=E-E_c$ and not by an even-function symmetry argument.

Inserting equation (12) in equation (6) to reduced

$$R_{CT}^{DA}(\epsilon)=\frac{2\pi}{\hbar}\int_{-\infty}^{\infty}\frac{|\langle V_{DA}\rangle|^2}{\sqrt{4\pi\lambda_{AD}k_BT}}e^{\frac{-(\lambda_{AD}+\Delta V^0+\epsilon)^2}{4\lambda_{AD}k_BT}}\varrho_a((E_c+\epsilon))\frac{l_e}{\sqrt[3]{\frac{6d_a^2}{\pi}}}d\epsilon \quad (13)$$

At equilibrium system, the activation density of state for system reduced to Fermi distribution function [22].

$$f(E)=\frac{1}{e^{[(\epsilon+E-E_F)/(k_BT)]}+1} \quad (14)$$

However, the Marcus–Gerischer model provided a good view of the electron transfer process between molecular electronic states and the continuum of available electronic states in semiconductors. According to this model, the charge transfer rate depends on several factors: coupling, reorganization energy, driving force, and the density of states (DOS) in the semiconductor, which itself depends on energy. This model does not inherently require a constant DOS; rather, this assumption is used as a simplifying approximation in current calculations.

Under the constant-DOS approximation, the Fermi-weighted activation density of states used in the present formulation is therefore

$$\varrho_a(E)=D_0f(E)=\frac{D_0}{\exp[(\epsilon+E-E_F)/(k_BT)]+1} \quad (15)$$

Using $E=E_c+\epsilon$, equation (15) becomes

$$\varrho_a(E_c+\varepsilon)=\frac{D_0}{e^{(\epsilon+E_c-E_F)/(k_BT)}+1} \quad (16)$$

Inserting equation (16) in equation (13) to obtained

$$R_{CT}^{DA}(\epsilon)=\frac{2\pi}{\hbar}\int_0^{\infty}\frac{|\langle U_{DA}\rangle|^2}{\sqrt{4\pi\lambda_{AD}k_BT}}e^{\frac{-(\lambda_{AD}+\Delta V^0+\epsilon)^2}{4\lambda_{AD}k_BT}}\frac{D_0}{e^{(\epsilon+E_c-E_F)/(k_BT)}+1}\frac{l_e}{\sqrt[3]{\frac{6d_a^2}{\pi}}}d\epsilon \quad (17)$$

The solution of integral in equation (17) is given results

$$R_{CT}^{DA}(\epsilon)=\frac{2\pi}{\hbar}\frac{|\langle V_{DA}\rangle|^2}{\sqrt{4\pi\lambda_{AD}k_BT}}e^{\frac{-(\lambda_{AD}+\Delta V^0)^2}{4\lambda_{AD}k_BT}}D_0\frac{l_e}{\sqrt[3]{\frac{6d_a^2}{\pi}}}k_BT\ln[1+\exp(\frac{E_F-E_c}{k_BT})] \quad (18)$$

The alternating harmonic series that appears in the original derivation is recovered only for the special energy reference $E_F=E_c$, Under this condition,

$$I_F=k_BT\ln 2. \quad (19)$$

Since [23].

$$\ln 2=1-\frac{1}{2}+\frac{1}{3}-\frac{1}{4}+\frac{1}{5}-\cdots=\sum_{n=1}^{\infty}\frac{(-1)^{n-1}}{n}, \quad (20)$$

it follows that

$$I_F=k_BT\sum_{n=1}^{\infty}\frac{(-1)^{n-1}}{n} \quad (21)$$

Substitution into equation (18) gives

$$R_{CT}^{DA}(\epsilon)=\frac{2\pi}{\hbar}\frac{|\langle V_{DA}\rangle|^2}{\sqrt{4\pi\lambda_{AD}k_BT}}e^{\frac{-(\lambda_{AD}+\Delta V^0)^2}{4\lambda_{AD}k_BT}}D_0\frac{l_e}{\sqrt[3]{\frac{6d_a^2}{\pi}}}\sum_{n=1}^{\infty}\frac{(-1)^{n-1}}{n}k_BT \quad (22)$$

Results

The calculated charge transfer rate $R_{CT}^{DA}$for the MK-2 dye/ InP semiconductor interface were obtained using the derived nonadiabatic electron transfer rate base on quantum theory. Calculation was performed using variety values for non-adiabatic coupling strength V_{DA} in range (0.1 to 0.4) eV taken from literature in Ref. [24] and taking four solvents environments: N,N-dimethylacetamide (DMAc), acetonitrile (ACN), methanol (MeOH), and 2,2,2-trifluoroethanol (TFE). The calculated charge-transfer rates for the MK-2 dye/InP semiconductor interface were obtained using the derived nonadiabatic electron-transfer rate equation based on quantum theory.

The reorganization energy (λ_{AD}) is a significant factor in the charge-transfer process from the excited MK-2 dye to the energy states of the InP semiconductor. The reorganization energy is calculated by various interfacial parameters, such as the radii of the MK-2 dye and InP semiconductor, the refractive index, the dielectric constant of the semiconductor, and the dielectric properties of the surrounding solvents. The radii of the MK-2 dye and the InP were determined by applying Equation (10), utilizing the molecular weight and density values of MK-2 from Table 1 and those of InP from Table 2. The resulting calculated radii were obtained as $7A^0$for MK-2 and $1.93\ \ A^0$ for InP.

The reorganization energy values were calculated using equation (9). This calculation incorporated the dielectric constant and refractive index of the InP semiconductor, as detailed in Table 2, along with those of the different solvents, as specified in Table 3. The resulting reorganization energy values for the examined solvent environments are presented in Table 4.

Table 1: Physical Properties of MK-2 Dye [25,26]

Property	MK-2 Dye
Chemical formula	$C_{58}H_{70}N_2O_2S_4$
Molecular weight	955.45 g/mol
CAS number	1037440-21-3
Type	Metal-free organic D–π–A sensitizer
Main structural units	Carbazole donor + quaterthiophene π-bridge + cyanoacrylic acid acceptor
Melting point	181–185 °C
Absorption maximum, λmax	480 nm
density	1.11 g/cm³
Molecular dimensions	26 × 13 × 7 Å
electrochemical potential	-0.89 V volts (V) with NHE

Table 2: Physical Properties of InP Semiconductor [27-28]

Property	InP value at ~300 K
Crystal structure	Zinc blende
Lattice constant	5.8687 A°
Density	4.81 g cm^{-3}
Molecular weight	145.792 g/mol
Band gap	1.344 eV
Electron affinity	4.38 eV
Static dielectric constant	12.5
Electron effective mass at Γ	7.29×10^{-32} kg
Effective conduction-band DOS	5.7×10^{17} cm^{-3}
Effective valence-band DOS	1.1×10^{19} cm^{-3}
Intrinsic carrier concentration	1.3×10^{7} cm^{-3}
refractive index	3.1
Thermal conductivity	0.68 Watt $m^{-1}K^{-1}$
atomic density of InP	3.97×10^{22} eV.cm^{-3}

Table 3: Physical Properties of Solvent [29]

Solvent	Chemical Formula	Relative Dielectric Constant (ε)	Refractive Index (n)
N, N-Dimethylacetamide (DMAc)	C_4H_9NO	37.8	1.438
Acetonitrile (ACN)	CH_3CN	35.9	1.344
Methanol (MeOH)	CH_3OH	32.7	1.329
2,2,2-Trifluoroethanol (TFE)	CF_3CH_2OH	26.7	1.291

Table 4: Calculation of Reorganization Energy λ_{AD}(eV) at the MK-2 Dye/InP Semiconductor Interface

Solvent	Chemical Formula	Relative Dielectric Constant (ε)	Refractive Index (n)	Reorganization Energy λ_{AD}(eV)
N,N-Dimethylacetamide (DMAc)	C_4H_9NO	37.8	1.438	0.344
Acetonitrile (ACN)	CH_3CN	35.9	1.344	0.388
Methanol (MeOH)	CH_3OH	32.7	1.329	0.393
2,2,2-Trifluoroethanol (TFE)	CF_3CH_2OH	26.7	1.291	0.408

The calculated reorganization energies (Table 4) increase in the order DMAc (0.344 eV) < ACN (0.388 eV) < MeOH (0.393 eV) < TFE (0.408 eV). This ordering does not follow the static dielectric constant alone, since DMAc has the highest ε (37.8) among the four solvents yet yields the lowest λ_{AD} while TFE has the lowest ε (26.7) yet yields the highest λ_{AD}. The trend instead follows the combined optical- and static-dielectric response embedded in equation (9), which depends on the difference between the inverse square of the refractive index and the inverse of the dielectric constant. TFE combines a comparatively low refractive index with a low dielectric constant, which enlarges this dielectric mismatch term relative to DMAc, where both the refractive index and dielectric constant are higher. The reorganization energy in this system is therefore governed by the contrast between the optical and orientational polarization response of the solvent rather than by solvent polarity in the conventional sense.

The electron injection kinetic energy is calculated as the difference between the LUMO (lowest unoccupied molecular orbital) level in the excited state of the dye and the minimum conduction band energy, using the vacuum energy scale using $\Delta V^0 = E_c - E_{LUMO}$ [30].

Depending on the energy level alignment [31-32] between the MK-2 Dye electronic level and the conduction band of InP, we calculate the driving force for charge-transfer at the

interface of MK-2 /InP which equals ΔV^0 =(-4.38) -(- 3.55) =-0.83eV

In the MK-2 dye/InP device, the density of states (DOS) is evaluated at a specific energy (0.83 eV) and treated as a constant in the simplified charge-transfer-rate model. This approximation is intended to represent the density of states locally at the chosen energy and does not imply that the density of states remains constant across the entire conduction band of indium phosphide (InP).

The interfacial charge-transfer kinetics between the excited MK-2 dye and the InP semiconductor can be analyzed within the nonadiabatic Marcus–Gerischer electron-transfer framework (equation 22), using the calculated reorganization energies (Table 4), the fixed driving force $\Delta V^0 = -0.83$ eV, and the InP conduction-band density of states, $D_0(E) = 1.326 \times 10^{20}$ eV^{-1} cm^{-3}.Using equation (22), the CT rate was calculated by incorporating the reorganization energies (λ_{AD}) obtained for the examined solvent environments, together with the driving force ($\Delta V^0 = -0.83$) and the conduction-band density of states of InP ($D_0 = 1.326 \times 10^{20}$eV^{-1} cm^3), Additionally, the electronic length $l_e = 3A^0$ [18] and all parameters take of a temperature 300 K using MATLAB software, in the charge-transfer rate equation. The electronic coupling parameter (V_{DA}) was varied from 0.10 to 0.40 eV to evaluate its influence on the interfacial electron-transfer kinetics.

The calculated Charge-Transfer Rate $R_{CT}^{DA}(\epsilon)$ values are summarized in Table (5), and the relationships between R_{CT}^{DA} and V_{DA}, as well as between R_{CT}^{DA} and λ_{AD}, are presented in figure (1) and (2).

Table 5: Charge-transfer rate ($R_{CT}^{DA}(s^{-1})$) values calculated for the MK-2/InP interface as a function of electronic coupling strength (V_{DA}).

V_{DA}(eV)	Charge-transfer rate $R_{CT}^{DA}(s^{-1})$			
	DMAc	Acetonitrile	Methanol	TFE
0.100	1.84×10^7	1.02×10^8	1.20×10^8	1.90×10^8
0.125	2.88×10^7	1.59×10^8	1.88×10^8	2.97×10^8
0.150	4.14×10^7	2.30×10^8	2.70×10^8	4.28×10^8
0.175	5.64×10^7	3.12×10^8	3.68×10^8	5.82×10^8
0.200	7.36×10^7	4.08×10^8	4.80×10^8	7.60×10^8
0.225	9.32×10^7	5.16×10^8	6.08×10^8	9.62×10^8
0.250	1.15×10^8	6.38×10^8	7.50×10^8	1.19×10^9
0.275	1.39×10^8	7.71×10^8	9.08×10^8	1.44×10^9
0.300	1.66×10^8	9.18×10^8	1.08×10^9	1.71×10^9
0.325	1.94×10^8	1.08×10^9	1.27×10^9	2.01×10^9
0.350	2.25×10^8	1.25×10^9	1.47×10^9	2.33×10^9
0.375	2.59×10^8	1.43×10^9	1.69×10^9	2.67×10^9
0.400	2.94×10^8	1.63×10^9	1.92×10^9	3.04×10^9

The dependence of R_{CT}^{DA} on the electronic coupling parameter V_{DA} is shown in Figure 1 for each solvent. In all four cases, R_{CT}^{DA} increases monotonically with V_{DA} over the examined range (0.10–0.40 eV). For DMAc, R_{CT}^{DA} increases from 1.84×10^7 s^{-1} at V_{DA} = 0.10 eV to 2.94×10^8 s^{-1} at V_{DA} = 0.40 eV, an approximately sixteen-fold increase corresponding to a fourfold increase in V_{DA}; the same ratio is reproduced for ACN, MeOH, and TFE (Table 5). This behavior is consistent with the $|V_{DA}|^2$ dependence predicted by nonadiabatic electron-transfer theory and the Fermi Golden Rule expression underlying equation (22): a rate proportional to the square of the electronic coupling matrix element. Physically, V_{DA} reflects the degree of orbital overlap between the excited-state wavefunction of MK-2 and the conduction-band states of InP at the interface, so an increase in V_{DA} corresponds to stronger electronic mixing between donor and acceptor states without altering the relative ranking of the solvent environments**,** which is instead determined by the reorganization energy and driving force, as discussed below.

A comparison of R_{CT}^{DA} among the four solvents (Table 5, Figure 1) shows that the solvent with the lowest λ_{AD} (DMAc) produces the lowest R_{CT}^{DA} at every value of V_{DA}, while the solvent with the highest λ_{AD} (TFE) produces the highest R_{CT}^{DA}. This trend, illustrated directly in Figure 2 for V_{DA} = 0.20 eV, is opposite to the behavior typically expected when the driving force is smaller than the reorganization energy. In the present system, however, $|\Delta V^0|$ = 0.83 eV is substantially larger than λ_{AD}across all four solvents (0.344–0.408 eV), placing the reaction in the Marcus inverted region.

In Marcus theory, the discrete transition rate reaches its maximum value when the change in Gibbs energy equals the reorganization energy. In exergonic processes, the state where the Gibbs energy is greater than the reorganization energy corresponds to the inverted region of that particular transition. However, in the Marcus–Gerischer framework, the electron transition rate at the interface between the MK-2 dye and the InP material depends on the alignment of the dye's energy levels and the band states of the InP, the density of states, and the Frankck–Condon weighting factor. The rate is obtained by incorporating the contributions from the available semiconductor states; therefore, the conventional anisotropy alone is insufficient to definitively determine that the rate lies within the inverted region. For the MK-2/InP device, the system classification within the inverted region must be supported by the system's alignment energy level, reorganization energy, and the evaluation of the Marcus-Gereicher equation. However, the requirement that the energy be greater than the reorganization energy is insufficient to describe the transition to the inverted region. Theoretically, the predicted that if the driving force increases so strongly that it becomes very negative (greater than the reorganization energy λ), then the electron's velocity begins to slow down instead of increasing.

In this regime, the activation term exp $[-(\lambda_{AD}+\Delta V^0)^2/4\lambda_{AD}k_BT]$ in equation (22) becomes less negative in its exponent as λ_{AD} increases toward $|\Delta V^0|$, so the activation barrier decreases and R_{CT}^{DA} increases with increasing λ_{AD}. Consequently, the solvent with the smallest reorganization energy does not yield the fastest charge-transfer kinetics in this system; rather, the position of λ_{AD}relative to the fixed driving force, not its absolute magnitude, determines the direction of the trend. Within the range of λ_{AD}values obtained here, all solvents remain on the ascending branch of the inverted-region rate profile, approaching but not reaching the activationless condition $\lambda_{AD} = |\Delta V^0|$. The conduction-band density of states of InP, $D_0(E)$, enters equation (22) as a multiplicative prefactor representing the number of accepting electronic states available at the energy corresponding to the driving force. Treating InP as a semiconductor with a continuous distribution of conduction-band states, rather than as a single discrete acceptor level, is necessary because the density of available states varies with energy above the conduction-band minimum, following the

$(E - Ec)^{(1/2)}$ dependence characteristic of a three-dimensional effective-mass conduction band. Since $D_0(E)$ was evaluated once, at the fixed energy offset $E - Ec = |\Delta V^0| = 0.83$ eV common to all solvents and coupling strengths, it acts as an overall scaling factor in the present calculations rather than a parameter distinguishing between solvents; its role is to establish the finite electron-accepting capacity of the InP conduction band at the relevant energy, rather than to introduce solvent-dependent variation in R_{CT}^{DA}.

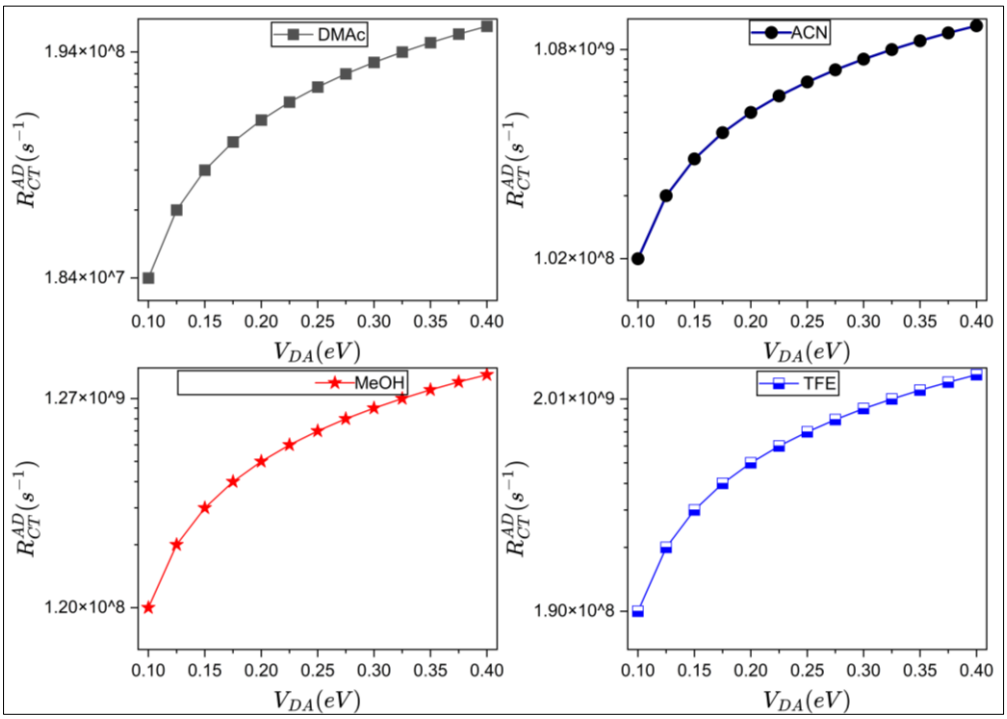


Fig 1: Dependence of the calculated charge-transfer rate R_{CT}^{DA} on the electronic coupling parameter V_{DA} for different solvent environments: (a) DMAc, (b) ACN, (c) MeOH, and (d) TFE.

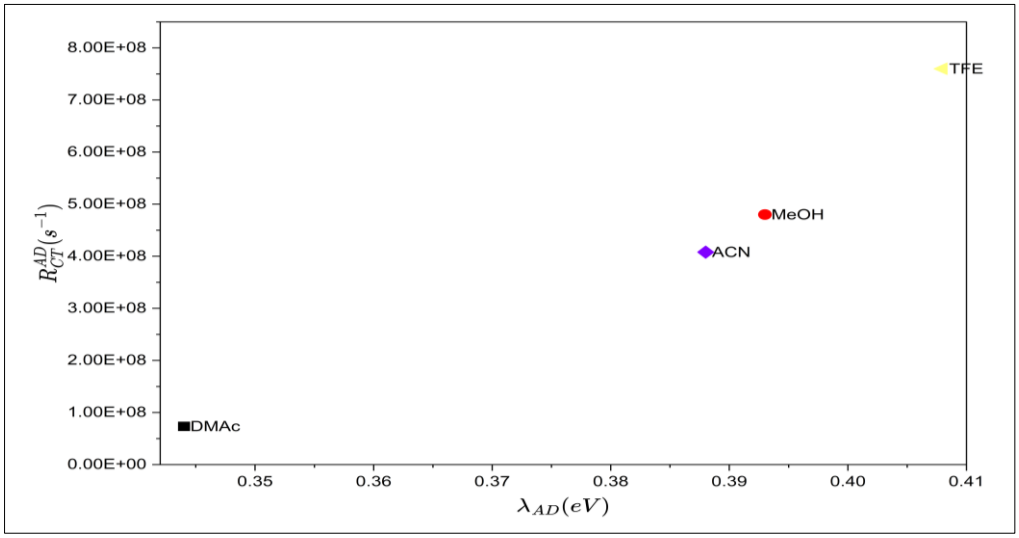


Fig 2: Relationship between the reorganization energy λ_{AD} and the calculated charge-transfer rate R_{CT}^{DA} at the MK-2/InP interface for $V_{DA} = 0.20\ eV$.

However, the reorganization energy λ_{AD} is relativeed by the charge-transfer rate R_{CT}^{DA} at the MK-2/InP interface for multi strength coupling values, Figure 2 show the relation between them at $V_{DA} = 0.20\ eV$.Taken together, the results indicate that interfacial charge-transfer kinetics at the MK-2/InP interface are governed by two largely independent factors within the Marcus–Gerischer formalism. Electronic coupling strength sets the absolute magnitude of R_{CT}^{DA} through a $|V_{DA}|^2$ scaling common to all solvent environments, while the solvent-dependent reorganization energy, combined with the fixed driving force, determines the position of the system along the Marcus rate–energy curve; because $|\Delta V^0|$ exceeds λ_{AD} for all solvents studied, this places the interface in the inverted region, where higher λ_{AD} corresponds to higher R_{CT}^{DA}. The InP conduction-band density of states, evaluated at the driving-force energy, provides a common prefactor reflecting the finite number of accepting states at that energy, without differentiating among

the solvent environments. The increasing electron transfer rates - the results of which are shown in Tables (5) and (6) - are consistent with the photovoltaic cell standards reported in the scientific literature [33].

Conclusion

A nonadiabatic Marcus– Gerischer electron-transfer model was applied to describe interfacial charge-transfer kinetics at the MK-2 dye/InP semiconductor interface, incorporating the conduction-band density of states of InP explicitly rather than treating the semiconductor as a single-level acceptor. The calculated charge-transfer rate was found to scale with the square of the electronic coupling parameter, $|V_{DA}|^2$, consistent with nonadiabatic electron-transfer theory, and this scaling was reproduced identically across all four solvent environments examined. The reorganization energy, calculated from the dielectric and refractive-index properties of the MK-2 dye, InP, and the surrounding solvent, ranged from 0.344 eV (DMAc) to 0.408 eV (TFE), following the dielectric mismatch between the optical and static solvent response rather than the static dielectric constant alone. Because the driving force for electron injection ($|\Delta V^o| = 0.83$ eV) exceeds the reorganization energy in every solvent considered, the interface operates in the Marcus inverted region, and the calculated charge-transfer rate increases, rather than decreases, with increasing reorganization energy -TFE yielding the highest rate and DMAc the lowest, at every electronic coupling strength examined. The conduction-band density of states, evaluated at the fixed driving-force energy, was shown to act as a common scaling prefactor reflecting the finite electron-accepting capacity of the InP conduction band rather than a solvent-differentiating factor. These findings indicate that the design and interpretation of dye/semiconductor interfaces for interfacial electron transfer cannot rely on reorganization energy or electronic coupling in isolation, but requires their joint evaluation relative to the driving force and the accepting semiconductor's density of states, particularly when the system operates outside the normal Marcus regime.

Acknowledgements

The Authors Have No Acknowledgements to Declare

Author Contributions

Declaration of Competing Interests

The authors declare that they have no known competing financial interests or personal relationships that could have appeared to influence the work reported in this paper.

References

1. Shen D, Chen WC, Lo MF, Lee CS. Charge-Transfer Complexes and Their Applications in Optoelectronic Devices. Mater. Today Energy, 20, 100644; 2021. doi:10.1016/j.mtener.2021.100644
2. Lekeufack Alongamo CI, Tasheh SN, Nkungli NK, Kogge Bine F, Ghogomu JN. Structural, Electronic, and Charge Transport Properties of New Materials Based on 2-(5-Mercapto-1,3,4-Oxadiazol-2-yl) Phenol for Organic Solar Cells and Light Emitting Diodes by DFT and TD-DFT. J. Chem. 2022;1802826(2022). doi:10.1155/2022/1802826
3. Baharfar M, *et al*. Gas Nanosensors for Health and Safety Applications in Mining. Nanoscale Adv., 5, 5997–6016; 2023. doi:10.1039/D3NA00507K
4. W. Wang, L. Luo, P. Sheng, J. Zhang & Q. Zhang. "Multifunctional Features of Organic Charge-Transfer Complexes: Advances and Perspectives." *Chem. Eur. J.*, 27(2), 464–490 (2021). https://doi.org/10.1002/chem.202002640.
5. Goetz KP, Vermeulen D, Payne ME, Kloc C, Jurchescu OD. Charge-Transfer Complexes: New Perspectives on an Old Class of Compounds. J. Mater. Chem. C, 2, 3065–3076; 2014. doi:10.1039/C3TC32062F
6. Raoufi M, *et al*. Influence of the Energy Level Alignment on Charge Transfer and Recombination at the Monolayer-MoS_2/Organic Hybrid Interface. J. Phys. Chem. C, 127, 5866–5875; 2023. doi:10.1021/acs.jpcc.2c08186
7. Z.-S. Wang *et al*. "Hexylthiophene-Functionalized Carbazole Dyes for Efficient Molecular Photovoltaics: Tuning of Solar-Cell Performance by Structural Modification." *Chem. Mater.*, 20(12), 3993–4003 (2008). https://doi.org/10.1021/cm8003276.
8. M. Gierszewski, A. Glinka, I. Grądzka, M. Jancelewicz & M. Ziółek. "Effects of Post-Assembly Molecular and Atomic Passivation of Sensitized Titania Surface: Dynamics of Electron Transfer Measured from Femtoseconds to Seconds." *ACS Appl. Mater. Interfaces*, 9(20), 17102–17114 (2017). https://doi.org/10.1021/acsami.7b03288.
9. Y. Q. Gao, Y. Georgievskii & R. A. Marcus. "On the Theory of Electron Transfer Reactions at Semiconductor Electrode/Liquid Interfaces." *J. Chem. Phys.*, 112(7), 3358–3369 (2000). https://doi.org/10.1063/1.480918.
10. Y. Q. Gao & R. A. Marcus. "On the Theory of Electron Transfer Reactions at Semiconductor/Liquid Interfaces. II. A Free Electron Model." *J. Chem. Phys.*, 113(15), 6351–6360 (2000). https://doi.org/10.1063/1.1309528.
11. Abd Ali NN, Al-Agealy HJM. Theoretical Calculations of the Current Density, Fill Factor and Efficiency of N749/TiO_2 Solar Cell. AIP Conf. Proc., 3036, 050005; 2024. doi:10.1063/5.0197418
12. Wang J, *et al*. Marcus Inverted Region of Charge Transfer from Low-Dimensional Semiconductor Materials. Nat. Commun., 12, 6333; 2021. doi:10.1038/s41467-021-26705-x
13. C. Coppola, M. Laura Parisi and A. Sinicrop,The Role of Organic Compounds in Dye-Sensitized and Perovskite Solar Cells, *Energies*,2023, 16(2), 573; https://doi.org/10.3390/en16020573
14. Gierszewski M, Glinka A, Ziółek M. Co-Sensitization Effects of Indoline and Carbazole Dyes in Solar Cells and Their Neutral–Anion Equilibrium in Solution. Materials. 2022;15(21):7725. doi:10.3390/ma15217725
15. A. Leo, F. Ambrosio, A. Landi & A. Peluso. "Electron Transfer Rates in Solution: Toward a Predictive First Principle Approach." *Chemistry*, 5(1), 97–105 (2023). https://doi.org/10.3390/chemistry5010008.
16. A. Leo & A. Peluso. "Electron Transfer Rates in Polar and Non-Polar Environments: A Generalization of Marcus' Theory to Include an Effective Treatment of Tunneling Effects." *J. Phys. Chem. Lett.*, 13(39), 9148–9155 (2022). https://doi.org/10.1021/acs.jpclett.2c02343.
17. Hashemi A, Peljo P, Laasonen K. Understanding Electron Transfer Reactions Using Constrained Density Functional Theory: Complications Due to Surface

Interactions. J. Phys. Chem. C, 127, 3398–3407; 2023. doi:10.1021/acs.jpcc.2c06537
18. Al Maadhede TS, *et al*. Effect of Solvents on Performance of Alq_3/ZnO Solar Cells: A Theoretical Approach. Energy Rep., 9(Suppl. 9), 427–434; 2023. doi:10.1016/j.egyr.2023.05.247
19. Fraggedakis D, *et al*. Theory of Coupled Ion-Electron Transfer Kinetics. Electrochim. Acta, 367, 137432; 2021. doi:10.1016/j.electacta.2020.137432
20. Saadon AK, Al-Agealy HJM. Study of Photoemission and Electronic Properties of Dye-Sensitized Solar Cells. Energy Rep., 6(Suppl. 3), 28–35; 2020. doi:10.1016/j.egyr.2019.10.015
21. Al-Obaidi SS, Al-Agealy HJM, Abbas SR. Theoretical Evaluation of Flow Electronic Rate at Au/TFB Interface. J. Phys. Conf. Ser., 1879, 032096; 2021. doi:10.1088/1742-6596/1879/3/032096
22. Lobato KPK. Charge Transport and Recombination in Dye-Sensitized Nanocrystalline Solar Cells. Ph.D. Thesis, University of Bath, Bath, UK; 2007.
23. J. Stewart. *Calculus: Early Transcendentals*, 8th ed., Cengage Learning, Boston (2016).ISBN: 9781285741550.
24. I. Azcarate, C. Costentin, C. Methivier, C. Laberty-Robert, and A. Grimaud. "Electron Transfer at the Metal Oxide/Electrolyte Interface: A Simple Methodology for Quantitative Kinetics Evaluation." J. Phys. Chem. C, 122(24), 12761–12770 (2018). https://doi.org/10.1021/acs.jpcc.8b02289
25. N. Koumura *et al*. "Alkyl-Functionalized Organic Dyes for Efficient Molecular Photovoltaics." *J. Am. Chem. Soc.*, 128(44), 14256–14257 (2006). https://doi.org/10.1021/ja0645640.
26. Soken Chemical, Engineering Co., Ltd. Organic Dye Sensitizer MK-2 for Dye-Sensitized Solar Cells (DSSC). Soken Chemical & Engineering Co., Ltd., technical product information, accessed September; 2026.
27. I. Vurgaftman, J. R. Meyer & L. R. Ram-Mohan. "Band Parameters for III–V Compound Semiconductors and Their Alloys." *J. Appl. Phys.*, 89(11), 5815–5875 (2001). https://doi.org/10.1063/1.1368156.
28. S. Adachi. *Properties of Group-IV, III–V and II–VI Semiconductors*, 1st ed., John Wiley & Sons, Chichester (2005). https://doi.org/10.1002/0470090340.
29. W. M. Haynes, ed. *CRC Handbook of Chemistry and Physics*, 94th ed., CRC Press, Boca Raton, FL (2013).
30. Y. Shen, L. Scudiero, and M. C. Gupta. "Temperature Dependence of Open-Circuit Voltage and UPS Study for P3HT:PCBM Organic Solar Cells." IEEE J. Photovolt., 2(4), 512–518 (2012). https://doi.org/10.1109/JPHOTOV.2012.2202877
31. AlHammade HTB. Theoretical Study of the Conduction Band and Energy Gap of GaInNAs/InP Quantum Well Structure. Nanomateriali, Nanotehnologii. 2022;20(1):15-23. doi:10.15407/nnn.20.01.015
32. M. Cheng, X. Yang, F. Zhang, and J. Zhao. "Tuning the HOMO and LUMO Energy Levels of Organic Dyes with N-Carboxomethylpyridinium as Acceptor To Optimize the Efficiency of Dye-Sensitized Solar Cells." J. Phys. Chem. C, 117(18), 9076–9083 (2013). https://doi.org/10.1021/jp311378b
33. A. Zdyb. "Current Status and Prospects for the Development of Emerging Photovoltaic Technologies." *Energies*, 19(14), 3299 (2026). https://doi.org/10.3390/en19143299

How to Cite This Article
Hassooni MA. Theoretical investigation of Charge-Transfer kinetics at the MK-2 Dye/InP semiconductor interface. J Front Multidiscip Res. 2026;7(2):444-451. doi:10.54660/.JFMR.2026.7.2.444-451.

Creative Commons (CC) License
This is an open access journal, and articles are distributed under the terms of the Creative Commons Attribution-NonCommercial-ShareAlike 4.0 International (CC BY-NC-SA 4.0) License, which allows others to remix, tweak, and build upon the work non-commercially, as long as appropriate credit is given and the new creations are licensed under the identical terms.